Chapter 8

Barkhausen Noise Experiments on Power Plant Steels

8.1 Experimental Method

8.1.1 Sample Preparation

The samples for BN testing were prepared as described in § 6.1. A 2% nital etch was used for the $2\frac{1}{4}$Cr1Mo steel samples, and a Kalling's No. 2 etch for the 11Cr1Mo samples.

8.1.2 Instrumentation

The BN measurements were taken at the University of Newcastle Design Unit under the supervision of Dr V. Moorthy, using a commercially available 'μSCAN 500' testing machine manufactured by Stresstech Oy - AST (Figure 8.1). Such instruments are used routinely in industry for a variety of nondestructive testing applications, such as detecting residual stresses at surfaces (Stresstech, WWW site). Figure 8.2 is a schematic diagram of the measurement system. The BN unit generates a sinusoidally varying current which, after amplification and filtration, is supplied to a coil wound around a yoke made of a ceramic ferrite material. The yoke is placed directly onto the sample, taking care to ensure good contact between the sensor and the surface. A pickup coil, wound around a core of the same ceramic ferrite, acquires the BN voltage signal, which is amplified and filtered. The unit is

connected to a standard PC with purpose-written software installed. This is used to control the magnetising current and analyse the output.

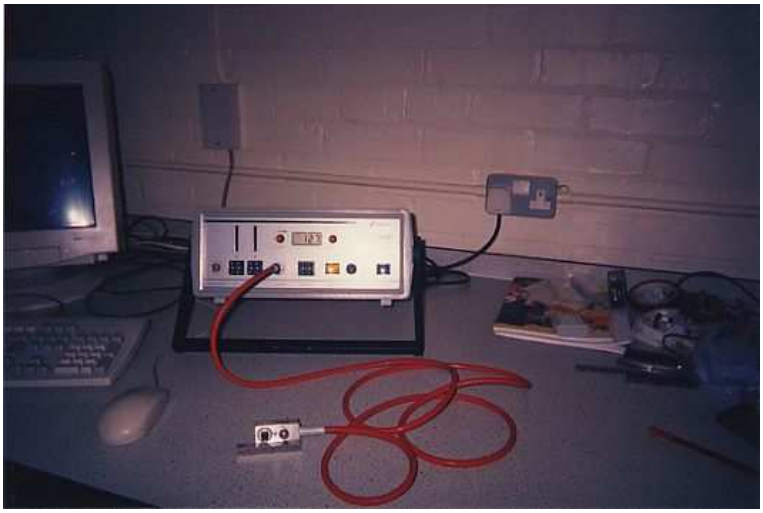

Figure 8.1: BN testing unit at the University of Newcastle.

The yoke and pickup apparatus constitute a commercially available sensor produced by the manufacturers of the BN unit (Figure 8.3). However, the core and the vertical pieces of the yoke can be removed and replaced.

8.1.3 Operating Conditions

Two modes of operation have been designed by the manufacturers of the instrument: 'microscan' and 'rollscan'. The former enables the application of excitation frequencies up to 125 Hz, and uses a hardware filter which allows output frequencies between 0.3 and 2.5 MHz. The latter permits excitation frequencies up to 30 Hz and output frequencies between 3 and 15 kHz. In this series of experiments, the 'rollscan' mode was used, with an excitation frequency of 4 Hz, since this was found by Moorthy *et al.* (2001) to give the optimal combination of signal amplitude and peak fine structure resolution on this instrument.

The applied magnetising current used was ± 0.7 A. (The instrument does not automatically translate this into an applied field.) A suitable signal

amplification, which gave a visible signal for the full range of samples investigated, was 30 dB. Signals obtained at different amplifications cannot be compared with complete certainty (Blaow, personal communication), so it was necessary to use the same value throughout.

Signal Analysis

Figure 8.4 is a screenshot showing the sinusoidal excitation current in blue, and the resulting noise signal in black. Data were acquired over four current cycles. In Figure 8.5, the rectified average of the forward (increasing-field) and reverse (decreasing-field) directions can be seen. Smoothed curves have also been plotted. The degree of smoothing can be controlled by the operator but in these experiments, the default settings were used.

The two smoothed signals are plotted on the same axes in Figure 8.6. The forward and reverse signals should be mirror images of one another. If there is asymmetry, this indicates that the sample was magnetised in one direction prior to testing. If this is the case, it is passed across a demagnetiser, which produces a rapidly oscillating field, several times and then the BN measurement is conducted again. If necessary, this process is repeated until a symmetrical signal is obtained (Moorthy, personal communication).

The software can be used to 'filter' the signal by displaying only the noise occurring within a particular frequency range. This facility was used for the analysis in § 8.3.

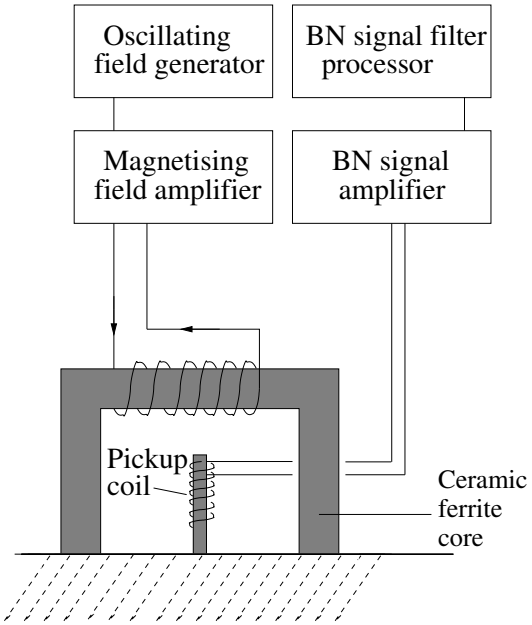

Figure 8.2: Schematic diagram of BN measurement equipment (after Blaow, 2001).

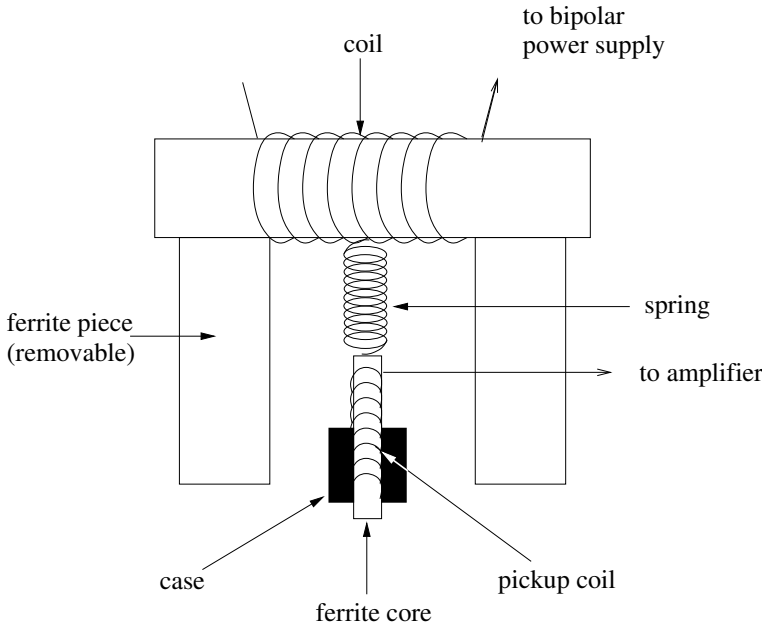

Figure 8.3: Schematic diagram of BN sensor.

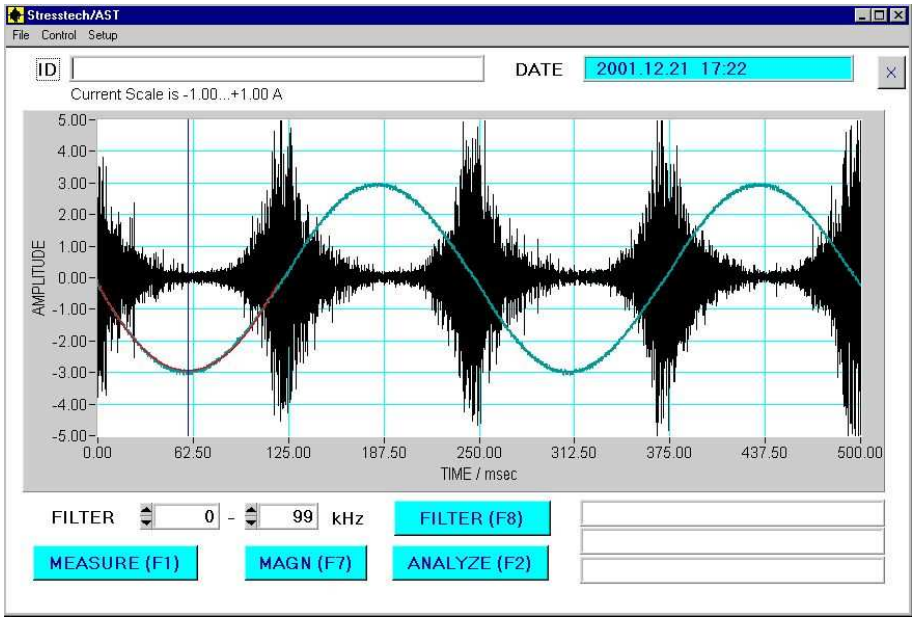

Figure 8.4: Screenshot from the software used at the University of Newcastle, showing the raw noise and magnetising current. This diagram and Figures 8.5 and 8.6 supplied by M. Blaow.

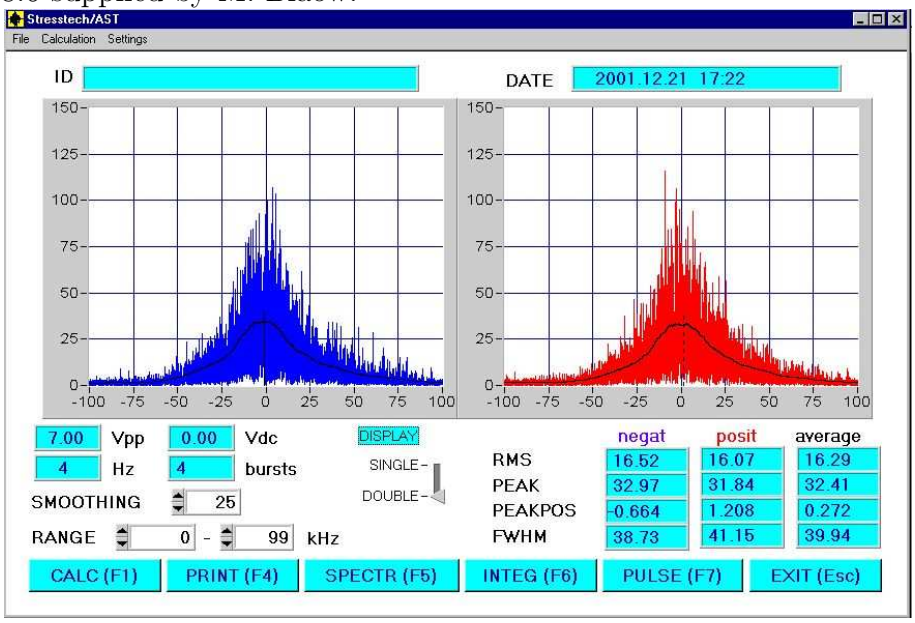

Figure 8.5: Screenshot showing the forward and reverse rectified BN.

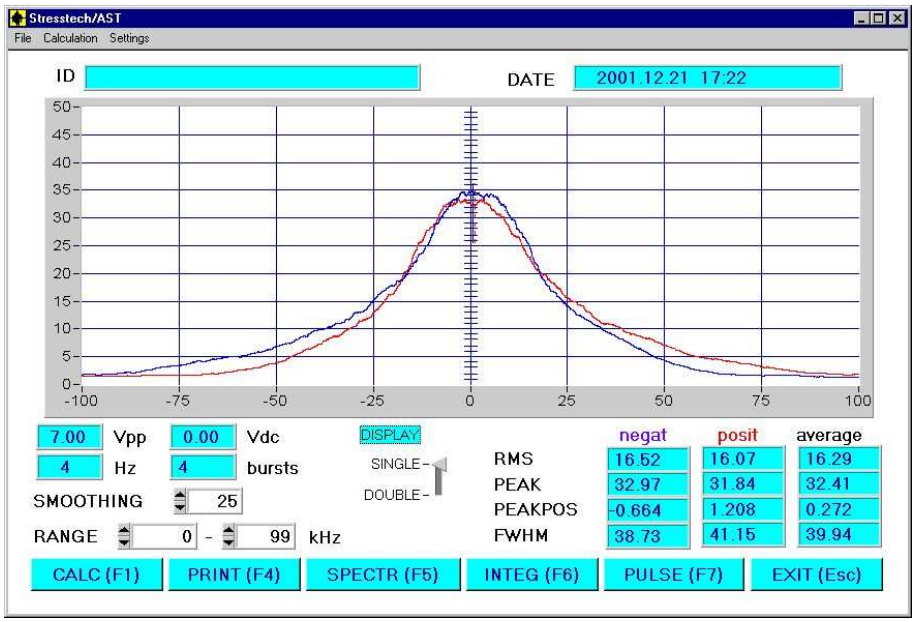

Figure 8.6: Screenshot showing the forward and reverse signals on the same axes.

8.2 Results

The rectified and smoothed BN signals were plotted against magnetising current for each of the samples tested. In each case, only the forward direction has been shown, since the reverse signal is almost identical. The scale on the horizontal axis is the applied magnetising current, and the vertical scale, quantifying the noise voltage, is given as a percentage of 5 V. These scales tend to be regarded as rather arbitrary, and not to be compared with the output from testing equipment with different geometries (Moorthy, personal communication).

500°C tempering

Figure 8.7 and Figure 8.8 show the BN signals for samples tempered at 500°C. On both graphs, the as-quenched (AQ) peak is shown for comparison.

For all the tempered specimens, the peaks are higher than for AQ. There appears to be a trend towards higher, narrower peaks with higher tempering time, but there is some scatter in this. The dramatic peak height increase between AQ specimens and those tempered even for a short time agrees well with the behaviour observed by Moorthy *et al.* in their tempering experiments. The onset of Barkhausen activity occurs at a lower current in the tempered sample than in the as-quenched sample in all cases.

Samples tempered for longer times (Figure 8.8) show much less variation in BN peak shape and position than those tempered for shorter times (Figure 8.7). In all the 500°C samples, an approximately symmetrical peak centred at a current of around 0.1 A is followed by a change in slope near 0.2 A, giving a gradual decrease of noise at high current.

600°C tempering

Figure 8.9 and Figure 8.10 show the noise signals from samples tempered at 600°C, with the AQ signal for reference. The maximum peak height observed in this series is larger than in the 500°C series.

The peak heights do not show much variation, apart from the peak at 256 hours, which is significantly higher than the others. The shape of the

32 hour peak seems anomalous.

The onset of noise occurs at a lower current in this set of samples than in the 500°C samples. The 600°C peaks are rather broader than the 500°C peaks, and enclose a larger area. However, the curve shapes may still be interpreted as an initial peak followed by a slope change to a less steep slope.

700°C tempering

Peaks from samples tempered at 700°C (Figure 8.11) are significantly broader than those from lower tempering temperatures; more activity occurs both at currents below zero and at high currents. There is no obvious trend between peak height and tempering time, or between peak position and tempering time.

Long-term 11Cr1Mo wt. % samples

The peak occurs at a noticeably higher current for the 11Cr1Mo samples (Figure 8.12) than for the tempered $2\frac{1}{4}$Cr1Mo steels, as illustrated by comparison with the $2\frac{1}{4}$Cr1Mo AQ peak. The peak heights are mostly smaller than those for tempered $2\frac{1}{4}$Cr1Mo steel, but there is no obvious systematic variation of height with tempering time.

8.2.1 Peak height, width and position

For each data set, the maximum height, the full width half maximum (FWHM), and the position on the applied current axis of the maximum height, were determined and plotted against tempering time (Figure 8.13, Figure 8.15 and Figure 8.17).

The Larson-Miller parameter P can be used to relate tempering time and temperature conditions on the same scale:

$$P = T(C + \log t) \tag{8.1}$$

where T is the absolute temperature (in K), t is the time in hours, and C is a constant with a value around 20.

The BN peak height, FWHM and position were plotted against P, which was calculated with $C = 16.7$ (Figure 8.14, Figure 8.16 and Figure 8.18).

There is no clear relationship between peak height and tempering time (Figure 8.13) but the $2\frac{1}{4}$Cr1Mo steel values increase approximately linearly with P, while the 11Cr1Mo values fall into a different regime (Figure 8.14). Similarly, there is a more obvious relationship of FWHM with P than with time, although some outliers are present (Figure 8.16).

The most obvious trend in these data is the decrease in peak position with P (Figure 8.18), which is followed by all the $2\frac{1}{4}$Cr1Mo steel values. The 11Cr1Mo steel values are again in a different regime.

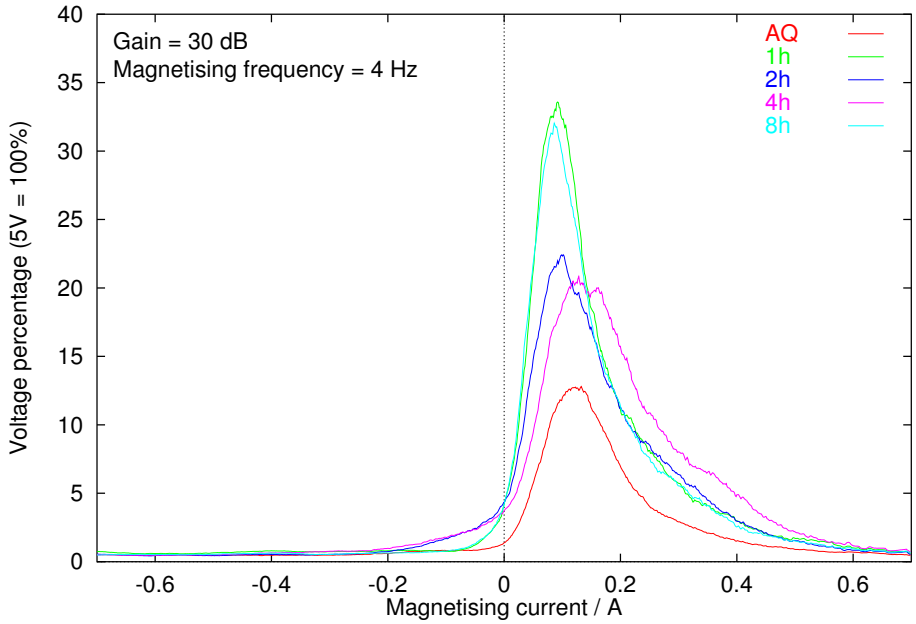

Figure 8.7: BN voltage versus magnetising current for samples tempered at 500°C (1–8 h).

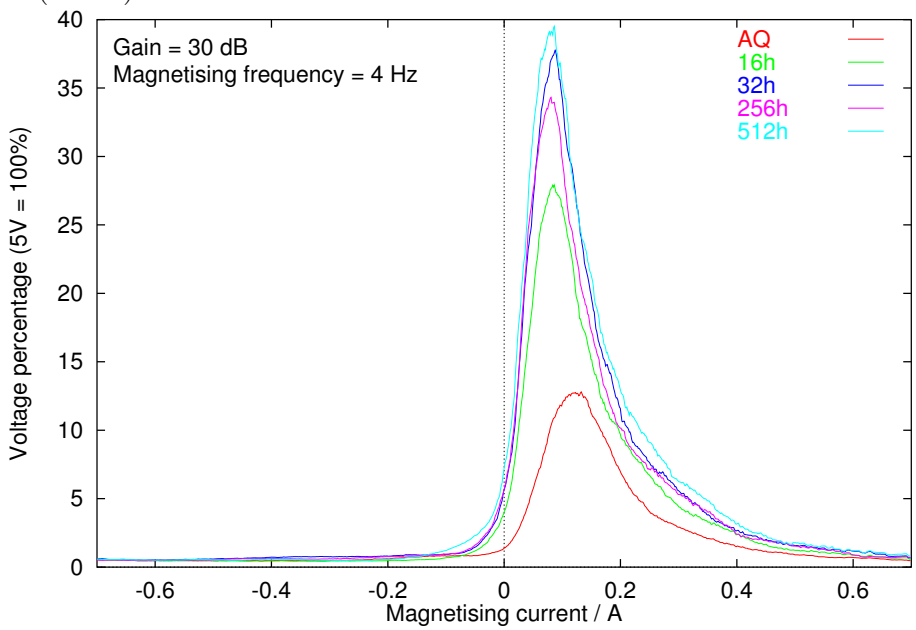

Figure 8.8: BN voltage versus magnetising current for samples tempered at 500°C (16–512 h).

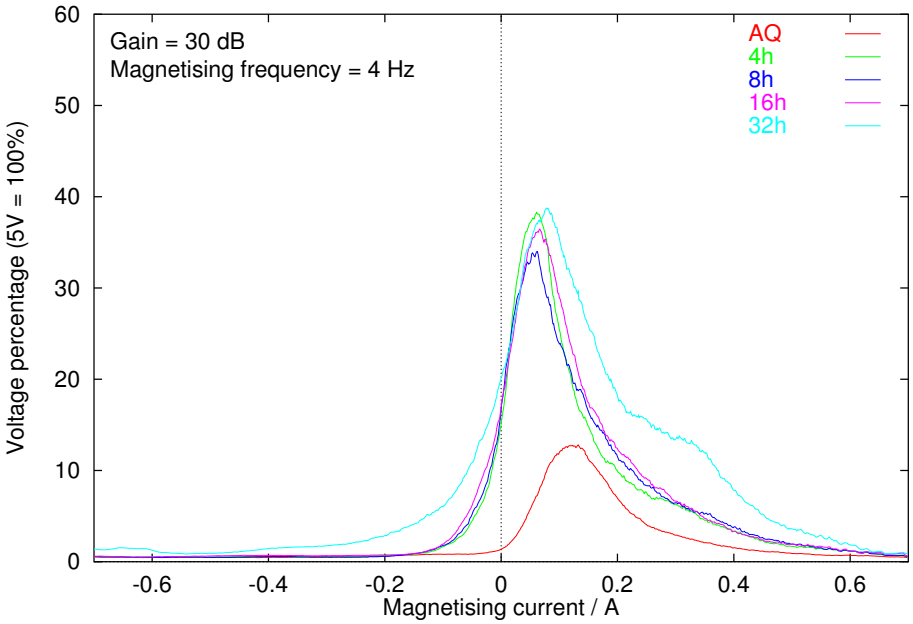

Figure 8.9: BN voltage versus magnetising current for samples tempered at 600°C (1–32 h).

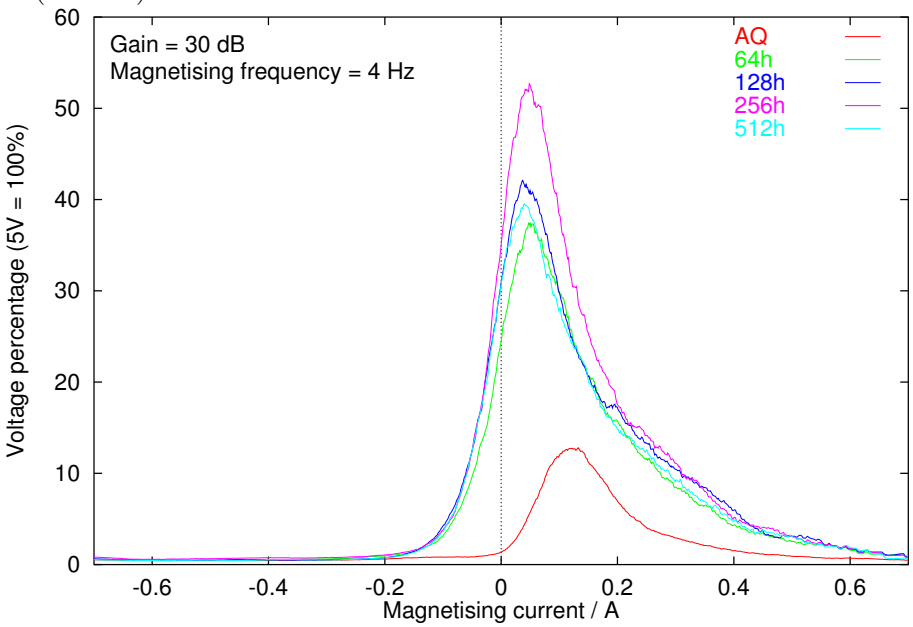

Figure 8.10: BN voltage versus magnetising current for samples tempered at 600°C (64–512 h).

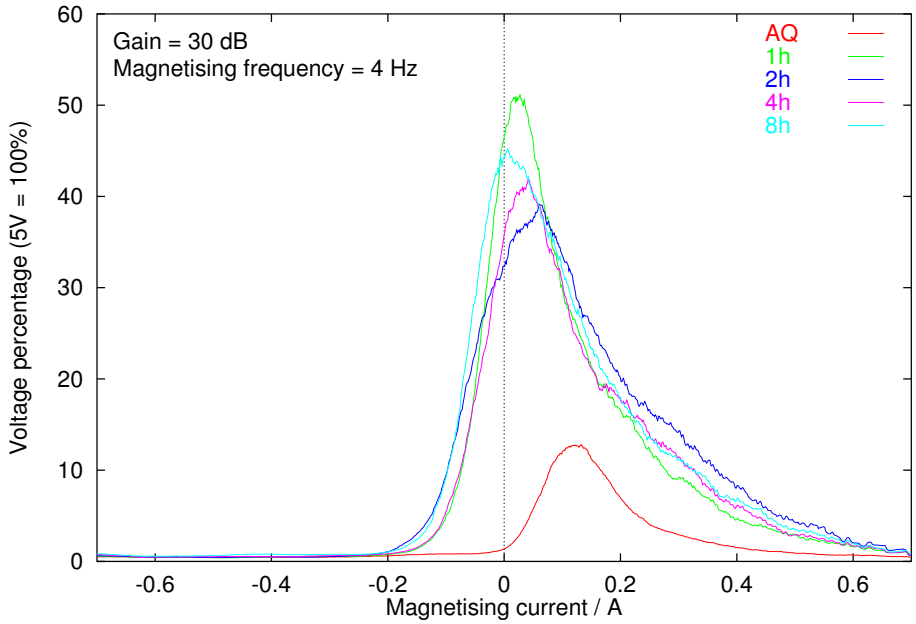

Figure 8.11: BN voltage versus magnetising current for samples tempered at 700°C.

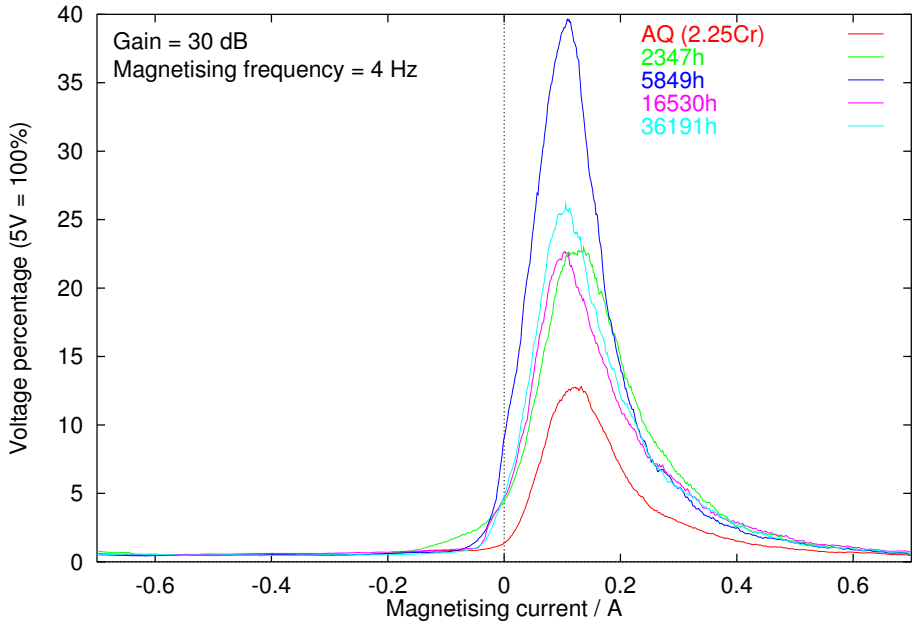

Figure 8.12: BN voltage versus magnetising current for 11Cr1Mo wt. % specimens.

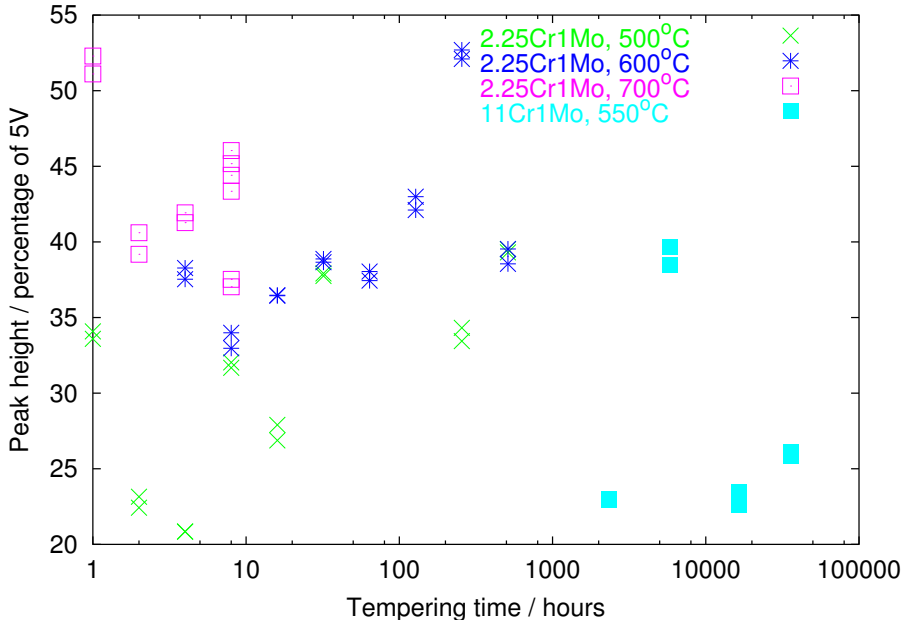

Figure 8.13: BN peak height versus tempering time.

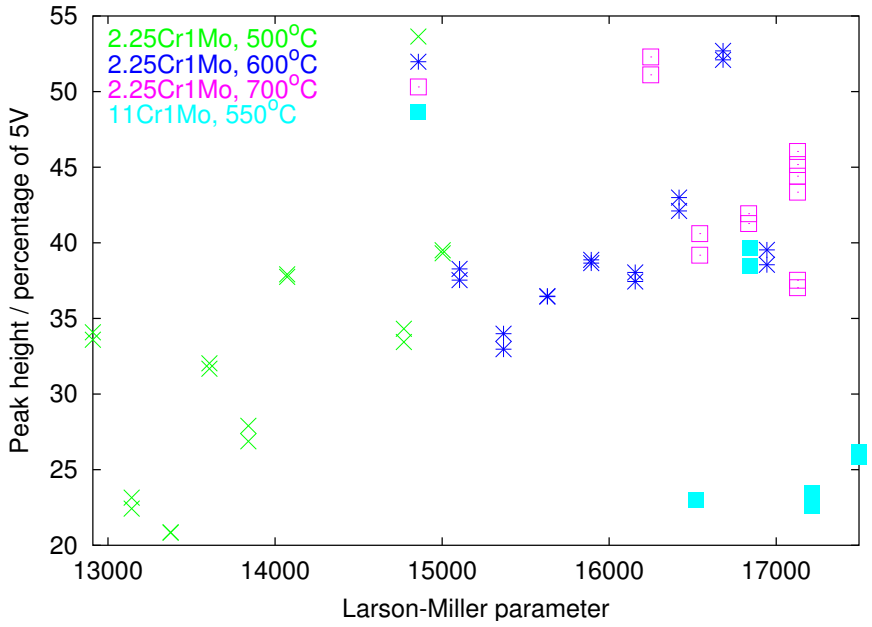

Figure 8.14: BN peak height versus Larson-Miller parameter.

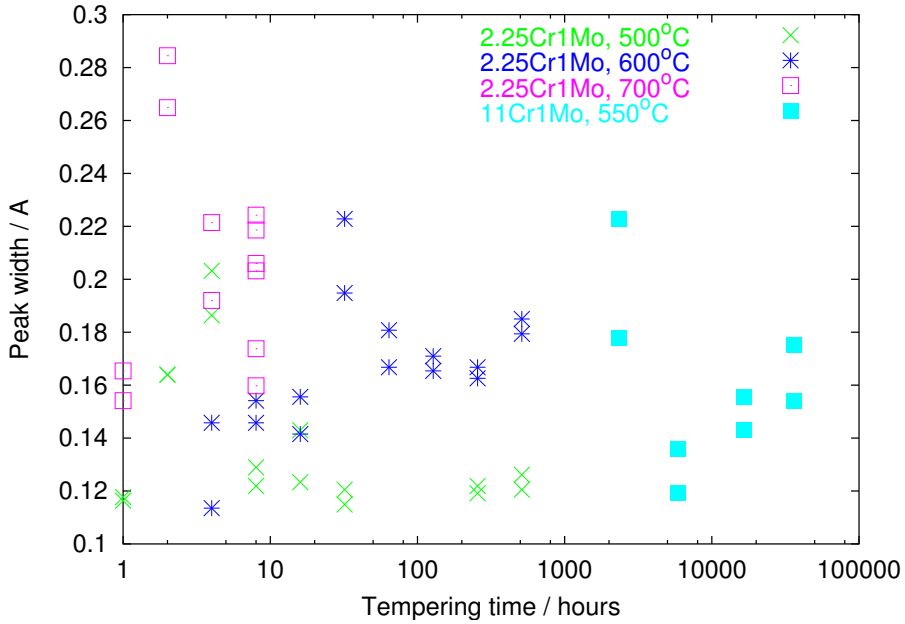

Figure 8.15: BN peak width (FWHM) versus tempering time.

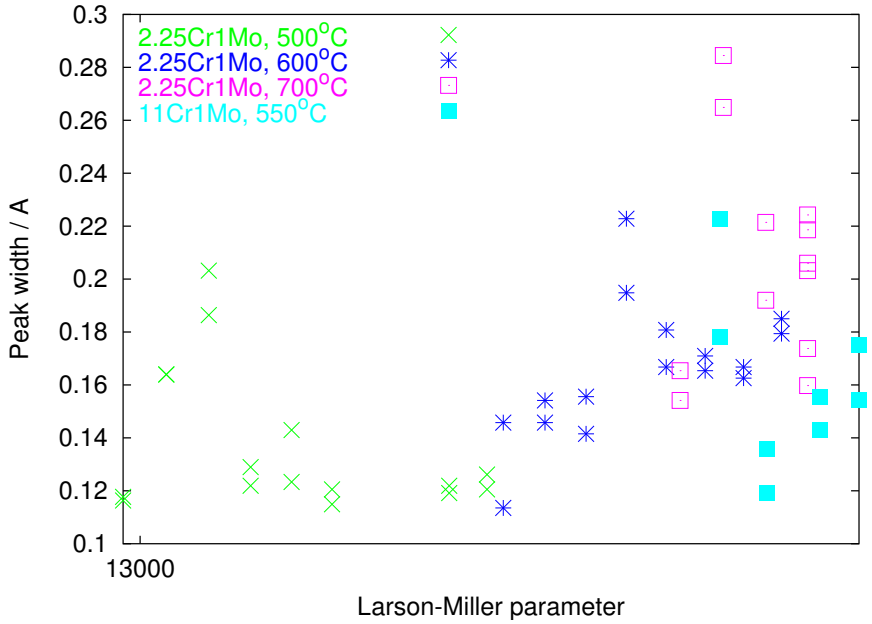

Figure 8.16: BN peak FWHM versus Larson-Miller parameter.

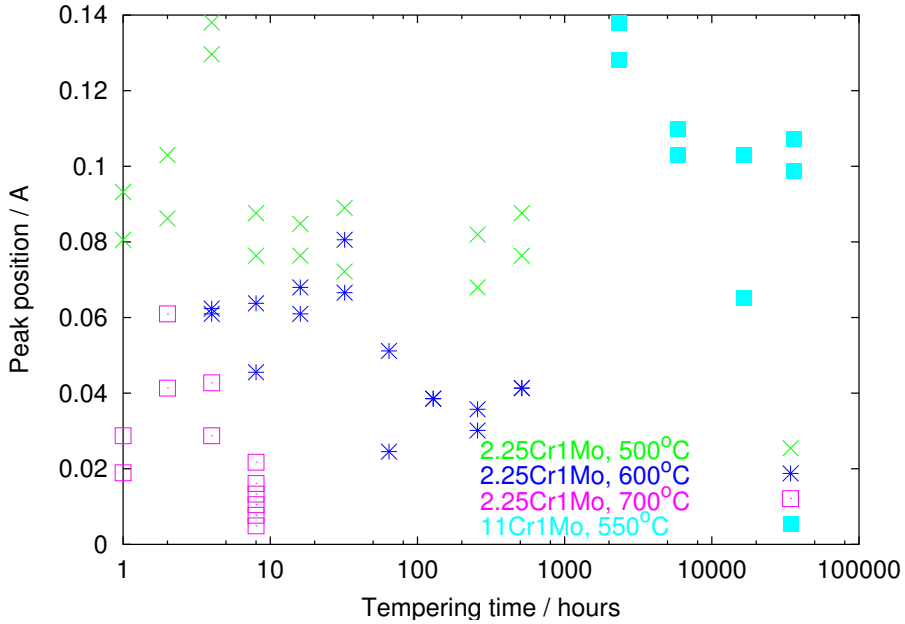

Figure 8.17: BN peak position versus tempering time.

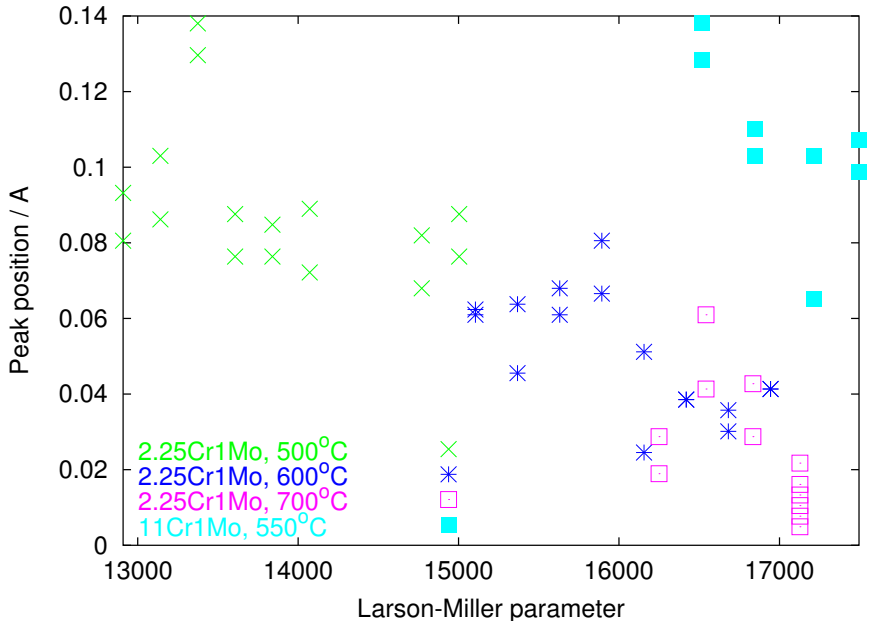

Figure 8.18: BN peak position versus Larson-Miller parameter.

8.2.2 Comparison with results of Moorthy *et al.*

Figure 8.19 shows a selection of the results obtained here together with some results on a $2\frac{1}{4}$Cr1Mo steel obtained by Moorthy *et al.* (1998, 2000) using apparatus of type (a) in Figure 4.2; the University of Newcastle apparatus is of type (b). The tempering temperatures are not the same in the two cases because the present work was intended to be complementary to those of Moorthy *et al.* rather than repeats of the same experiments. Also, Moorthy *et al.* did not quench their samples. The actual amplitudes of the noise signals measured depend on such factors as experimental geometry and signal amplification, so it is not possible to compare the values directly, and they are plotted on different vertical axes. However, the range of values on the horizontal axis should be the same since the current varies within the same range.

In the results of Moorthy *et al.*, the noise peaks occur at higher currents. The two sets of results are consistent in that the peak becomes higher, and moves to a lower current, after tempering. The change in height on tempering is more pronounced in the results of Moorthy *et al.* than in this study. The AQ peak from this study and the normalised peak of Moorthy *et al.* are similar in shape, but the tempered sample peak shapes in the present study are much less symmetrical than the Moorthy *et al.* peaks. The peak height changes seen by Moorthy *et al.* are much more dramatic than those in Figure 8.9, Figure 8.10 and Figure 8.11. Some of these differences can be accounted for by the greater severity of tempering in the Moorthy *et al.* experiment[1]. However, the comparative positions of the AQ and normalised peaks suggest that there is also some influence from the apparatus configuration.

The double-peak behaviour observed by Moorthy *et al.* at long tempering times is completely absent in all the measurements made in this study. This may be because 600°C is too low a temperature to produce this behaviour even at long tempering times, while the tempering at 700°C was carried out

[1]The highest Larson-Miller parameter value in the Moorthy *et al.* study was just under 18000, whereas the highest value in the present study was 17000.

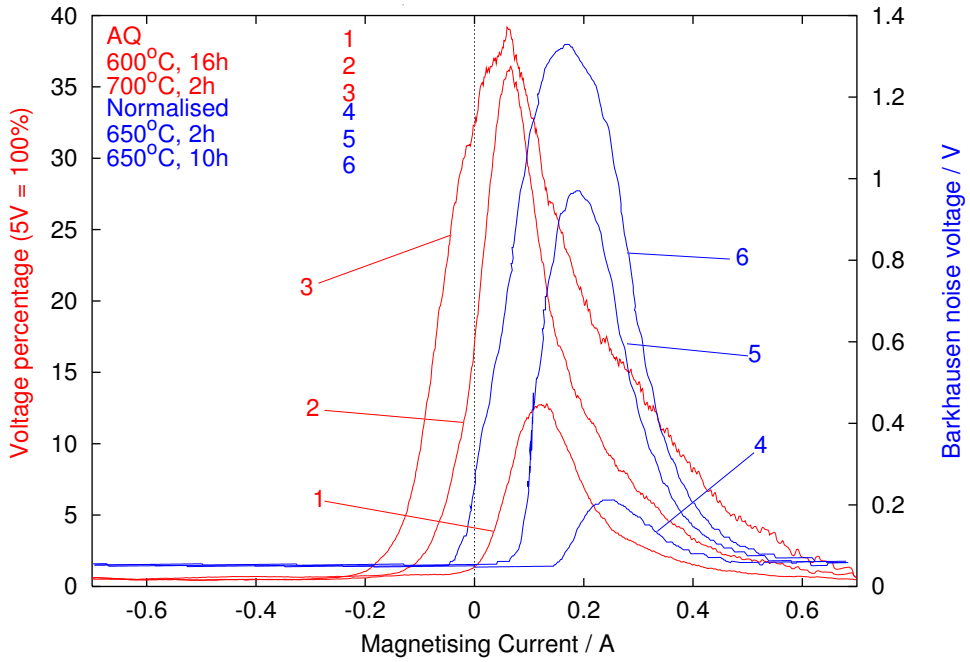

Figure 8.19: A comparison between results obtained in this study (red) and results obtained by Moorthy *et al.* (1998, 2000) (blue).

for too short a time for double peaks to be seen. An alternative explanation is that double-peak behaviour should be present in some of the samples, but it is suppressed because the noise contributing to the second peak is at a frequency which is filtered out. Previous work at the University of Newcastle using this apparatus suggests that the second explanation is possible (Blaow, personal communication).

8.2.3 Experiments on tempered plain-carbon steel

Double-peak behaviour in tempered plain-carbon steels has been observed in a number of investigations (Buttle *et al.*, 1987c; Kameda and Ranjan, 1987a; Moorthy *et al.*, 1998). The capacity of this apparatus to detect a second peak can therefore be tested using samples of a steel which is known to produce double peaks when tested with other apparatus.

Three samples of a water-quenched 0.1 wt. % C steel were tested. One

of these had been tempered for 0.5 hours, and another for 100 hours. Two measurements were taken on each sample. In Figure 8.20, a clear difference in peak position can be seen between the AQ and the tempered samples. There is no second peak visible in any of the signals, but the tempered samples show a slope change, which is absent in the AQ signal, after the initial peak. This may be equivalent to the slope changes seen in the tempered $2\frac{1}{4}$Cr1Mo steels: the only manifestation of high-current activity visible with this apparatus.

It is interesting to note the large difference in peak height from the two measurements on the AQ sample. This may be due to large-scale inhomogeneities in the AQ microstructure such as those observed using OIM (Chapter 7), or it may be indicative of a lack of repeatability with this apparatus.

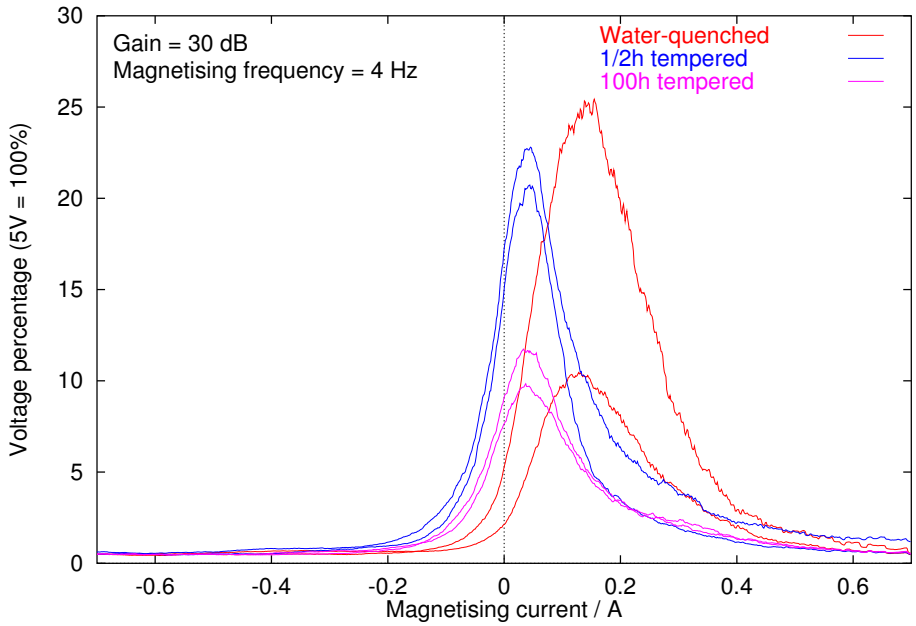

Figure 8.20: Plain-carbon steel tempering

The evidence from this experiment supports the suggestion that the apparatus would suppress any double peaks which should be present. However, this does not in itself confirm that a given sample should display a second peak as opposed to a change in slope. In order to investigate this question, the noise frequency of different samples and the shape of the noise signal

within particular frequency ranges was investigated.

8.3 Frequency analysis

The filtering hardware used by the Barkhausen measurement system in the 'rollscan' mode suppresses frequencies above 15 kHz and below 3 kHz, using a trapezium-shaped filter (Figure 8.21). However, it is believed that some interesting microstructural information is contained in the part of the signal below 3 kHz (Moorthy, personal communication).

Frequency content of the noise signal

Figure 8.22 shows the signals for the AQ sample and the shortest and longest tempering times at 500 and 700°C. The 'amplitude' on the vertical axis is the sum of the amplitudes of all the noise pulses occurring at a particular frequency.

For all the samples, the signal reaches its greatest amplitude near the centre of the unfiltered region (3–15 kHz). There is almost no noise at frequencies below 1 kHz, then a sharp peak at around 2 kHz. This occurs in all BN measurements and is believed to be an artefact of the measuring process (Moorthy, personal communication). The noise amplitude increases steeply between 2 and 3 kHz but decreases much more slowly beyond 15 kHz. The AQ signal has the smallest amplitude throughout the frequency range. For 500°C tempering, the amplitude is higher but there is no noticeable difference between the longer and shorter tempering times. The 700° samples have a higher amplitude, and a small amplitude increase is visible between the 1 hour and 8 hour data. Yamaura *et al.* (2001), in a similar analysis on pure iron, observed large peaks at 3 and 60 kHz but no such structure is visible here, possibly because of the narrowness of the filtering window.

It appears that frequencies below 3 kHz are more severely attenuated than those above 15 kHz with this filter. The discrepancies between the data obtained with this apparatus and those in the literature are therefore probably attributable mainly to the absence of the lower-frequency part of the signal.

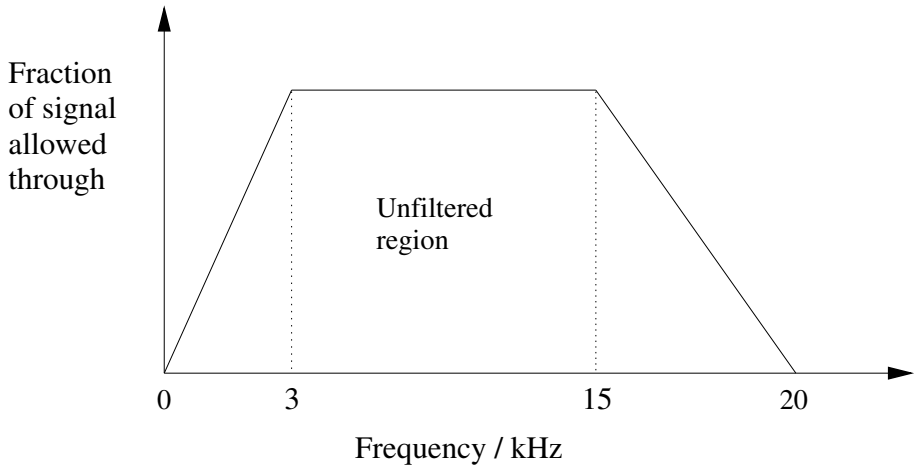

Figure 8.21: Frequency filter in 'rollscan' mode (Blaow, personal communication).

Signal analysis in narrow frequency ranges

Moorthy *et al.* (2001) noted the lack of the expected second peak in quenched and tempered 0.1 wt. % C steel using this apparatus, and analysed the signal within narrow frequency ranges to study the low-frequency noise. A clear second peak was visible in the tempered steel in the range 4–5 kHz, while only a single peak was seen in the AQ sample at all frequencies.

The signals from the 600°C $2\frac{1}{4}$Cr1Mo steel samples were analysed in a similar way to test whether a second peak was visible at low frequencies. The first analysis considered noise with frequencies between 0 and 3 kHz. The signal amplitude was low, owing to filtering, so the highest available amplification, 99 dB, was applied. Figure 8.23 shows some evidence of a second peak centred around a current between 0.3 and 0.4 A; this is particularly prominent in the 256 h signal. However, some evidence of activity at 0.4 A is also visible in the AQ sample, which should have only a single peak. The large peak, although at a similar position to the peaks in Figure 8.9 and Figure 8.10, is narrower and more symmetrical.

Setting the upper frequency limit to 5 kHz (Figure 8.24) gives peaks which more closely resemble those in Figure 8.9 and Figure 8.10. However, there

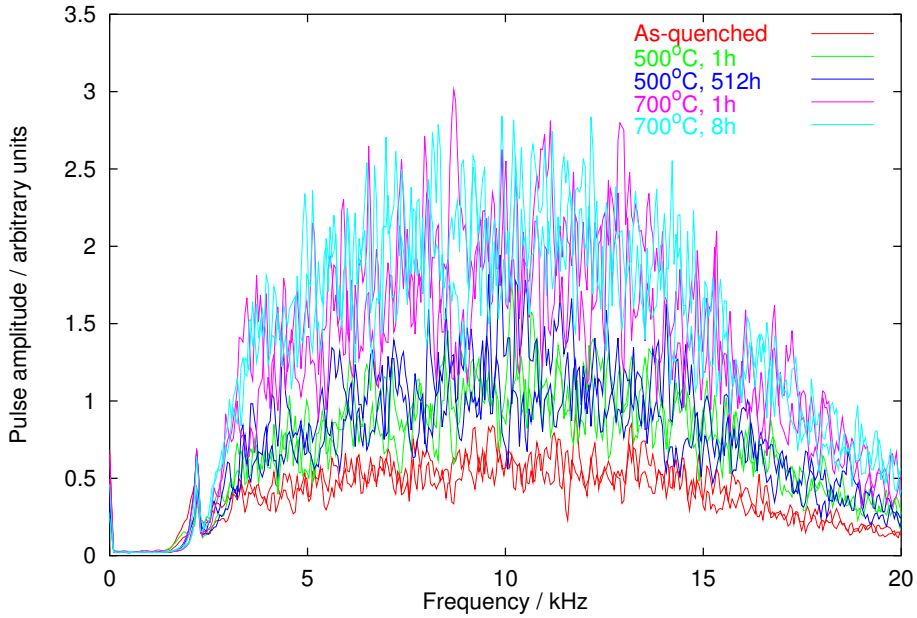

Figure 8.22: Frequency content of various noise datasets

is still evidence of activity in the high-current region. A clear slope change is visible in some peaks, notably those corresponding to shorter tempering times.

Analyses of frequencies within narrower ranges for individual samples are shown in Figure 8.25 (4 hours, 600°C) and Figure 8.26 (8 hours, 600°C). In both, a large, broad, high-current peak is visible for frequencies below 1 kHz. However, its smooth shape, compared to the typical roughness of the other curves, suggests that it may be an artefact of the measuring and filtering system rather than a true noise measurement. Double peaks or pronounced slope changes are visible in the 2–3 and 3–4 kHz ranges for both samples.

In Figure 8.27 (256 hours, 600°C) and Figure 8.28 (512 hours, 600°C), comparison between the signal content in the 0–3 kHz and the 0–5 kHz ranges can be seen. From the shape change between the two ranges, it is evident that there is significant activity in the range 0.2–0.4 A between 3 and 5 kHz.

These results strongly suggest that the low-frequency ranges do contain useful information, especially from events occurring at high applied currents.

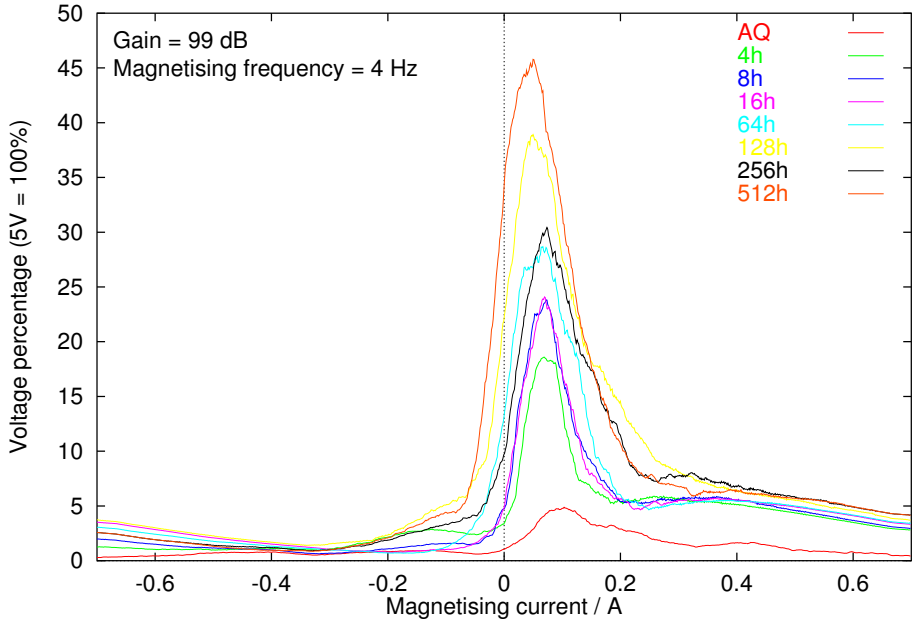

Figure 8.23: 0–3 kHz component of Barkhausen signal for 600°C tempered steels.

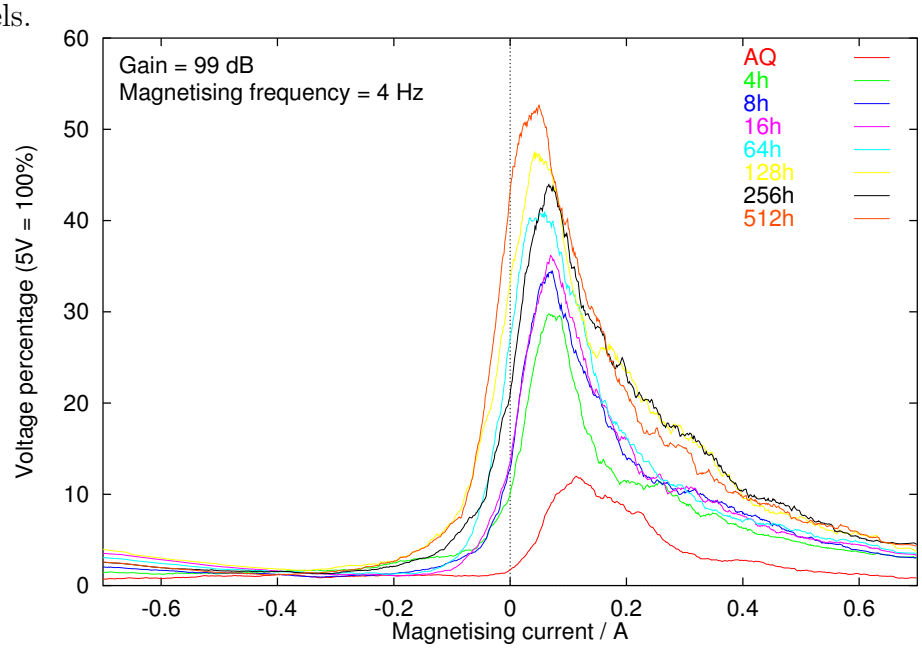

Figure 8.24: 0–5 kHz component of Barkhausen signal for 600°C tempered steels.

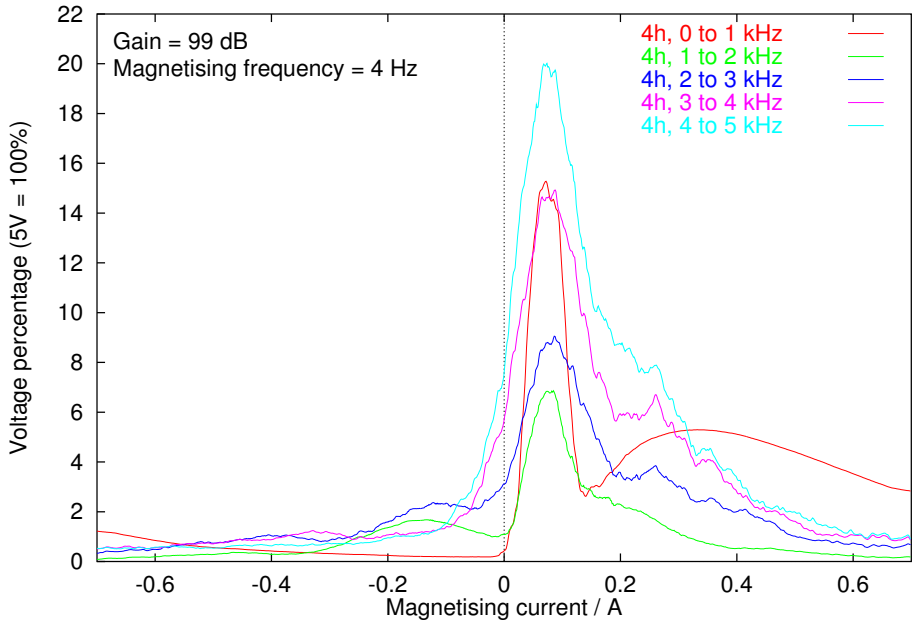

Figure 8.25: 600°C, 4 hour tempering: signals obtained from different frequency ranges.

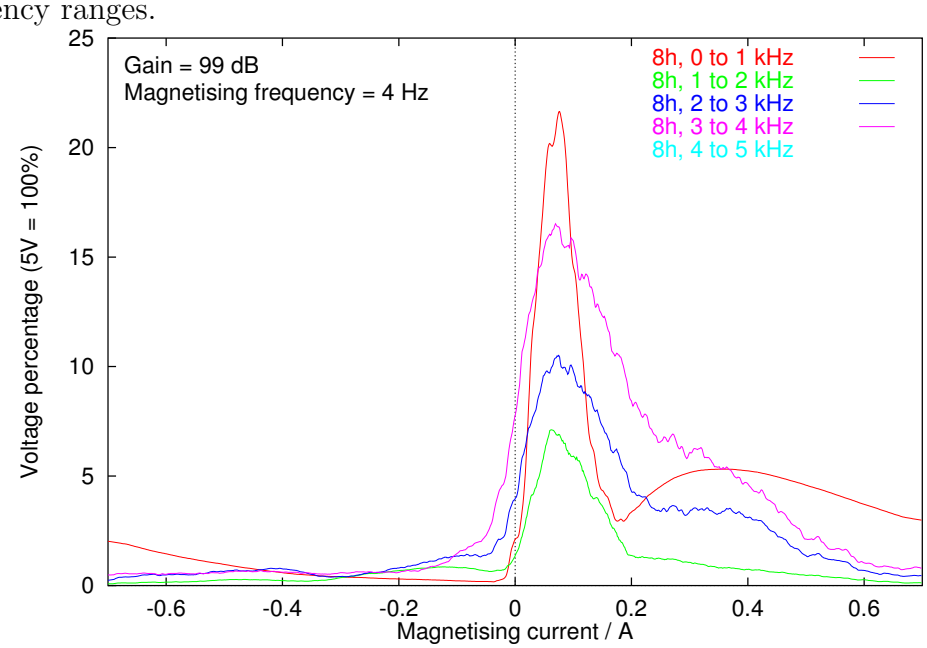

Figure 8.26: 600°C, 8 hour tempering: signals obtained from different frequency ranges.

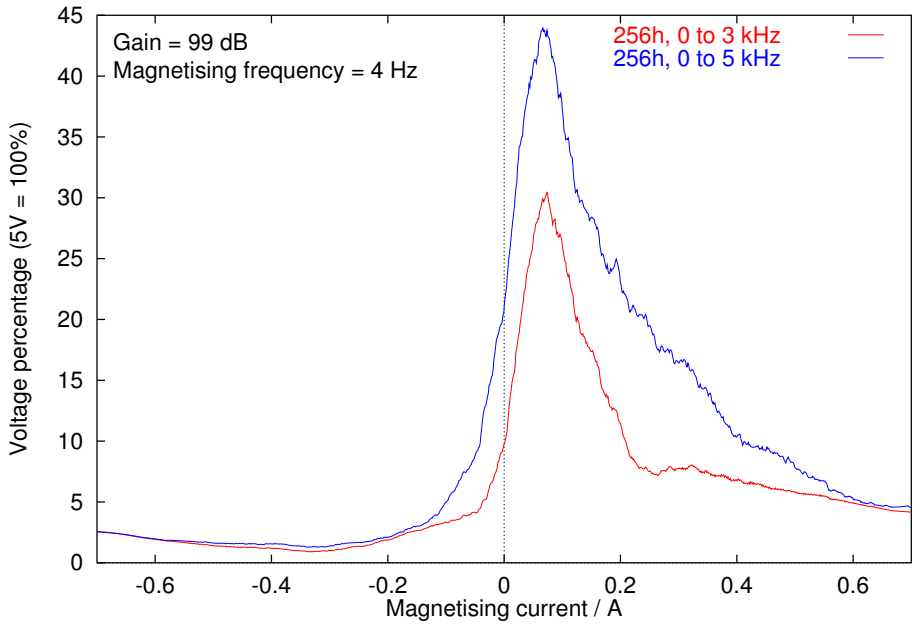

Figure 8.27: 600°C, 256 hour tempering: comparison of 0–3 kHz and 0–5 kHz ranges.

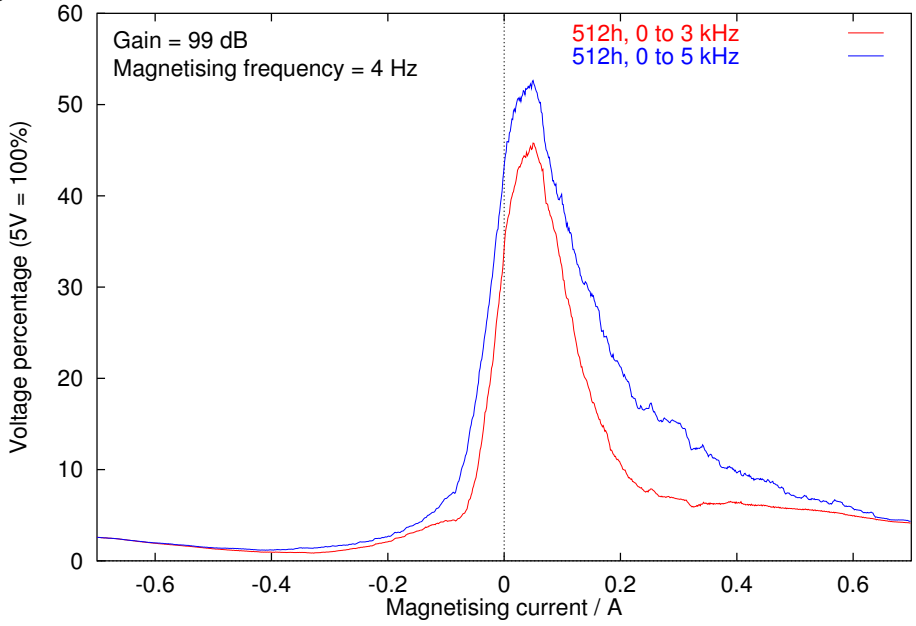

Figure 8.28: 600°C, 512 hour tempering: comparison of 0–3 kHz and 0–5 kHz ranges.

8.3.1 Checks on validity of results

Repeatability

Repeat measurements were taken on selected samples to determine the intrinsic experimental variability of the measurement system. Figure 8.29 shows both the forward and the reverse parts of three measurements from the same sample (8 hours, 700°C). The peak position and shape are consistent between measurements, but the peak height appears more variable. The overall range of peak heights observed in tempered $2\frac{1}{4}$Cr1Mo steels is 20–55 units on the vertical scale, but it appears from Figure 8.29 that variations can occur over almost a third of this total range.

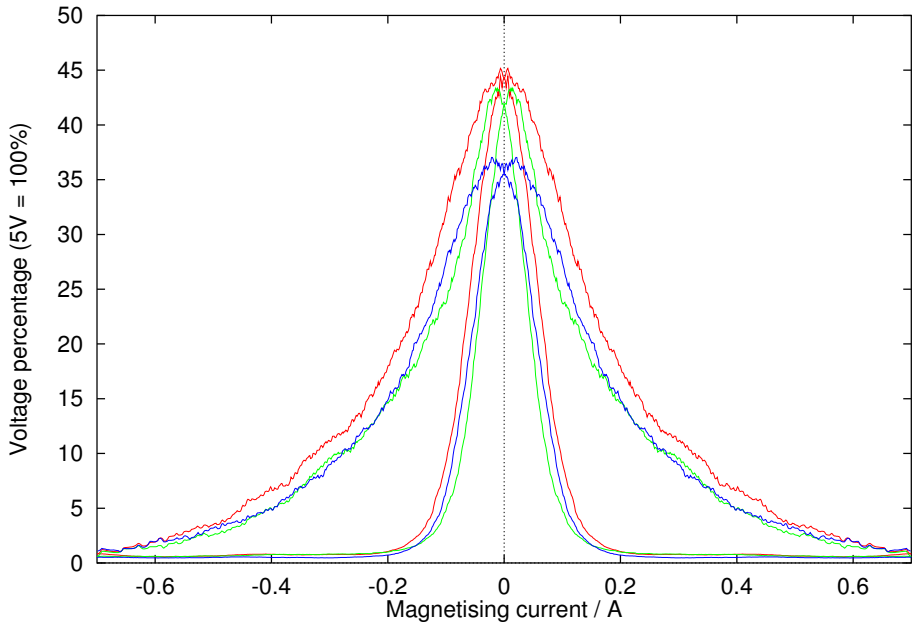

Figure 8.29: Repeatability study on sample tempered at 700°C for 8 hours.

Ferrite probe geometry

The original ferrite pole pieces for this apparatus were rectangular in section, but subsequently the effect of using round-ended pieces was investigated (Blaow, personal communication). These gave better repeatability, which was attributed to the smaller contact area. However, more recently,

a new set of rectangular-section pieces, with improved grinding, have been found to give good results; these last were used for the experiments described in this chapter. It now appears that the more critical part of the apparatus is the pickup coil core, which should be ground to a smooth shape to give good signal quality (Blaow, personal communication). Since this requires manual grinding, which is a difficult procedure, the scope for improvements is limited.

Figure 8.30 is a comparison of the signals obtained from the same sample (512 hours, 500°C) using three sets of pole pieces. The data from the new pieces were acquired using a higher amplification and are therefore plotted on a different scale on the right-hand vertical axis. The new pieces give a smoother curve, and better agreement between forward and reverse signal shapes. It is noticeable that, for the round-ended pieces, the peak position is different and the peak is broader than in the other cases.

Although it is difficult to tell what constitutes a 'better' or 'more accurate' signal without an external point of reference, it is reasonable to expect that greater smoothness and symmetry between forward and reverse directions is indicative of a more even acquisition of noise pulses. Whether or not this is the case, it is clear that the observed signal is sensitive to the shape and grinding quality of the pieces. Another issue which may contribute to the differences seen in Figure 8.30, however, is that the technique of taking Barkhausen measurements requires some skill and practice. The data from the new probe were obtained later than those from the other two probes, so this could be part of the reason for the improved smoothness.

Overall magnetising geometry

It would be useful to investigate whether the difference in geometry between the contact-type sensor used here, and the yoke-type apparatus used in much of the previous work in this field, gives any systematic differences in results. However, such a comparison is not possible unless the filtering applied in the two systems is the same. New measurement apparatus of both geometries is currently being constructed at the University of Newcastle in order to investigate this question.

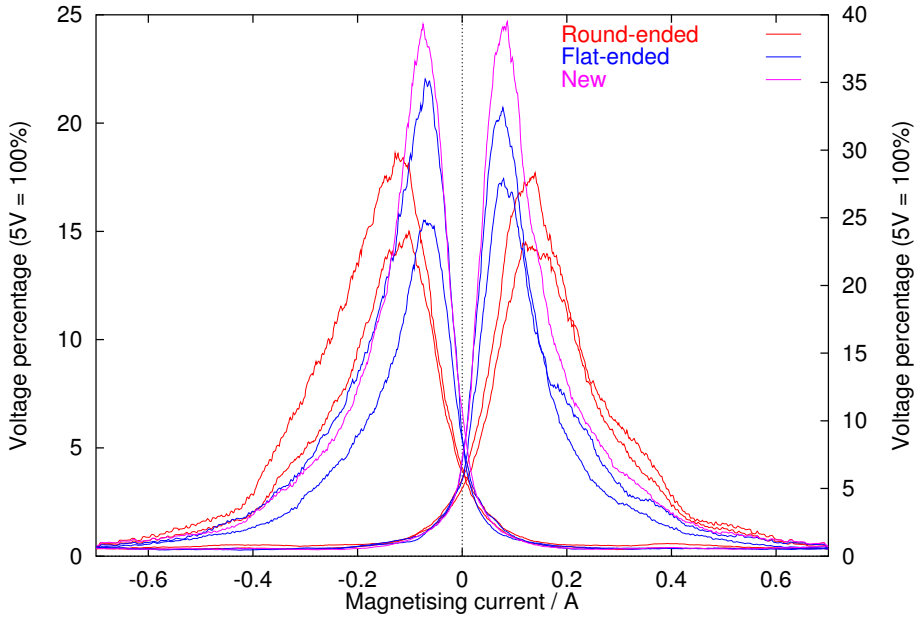

Figure 8.30: Effect of different pole-piece shapes on the 500°C, 512 hours signal.

8.4 Discussion

8.4.1 Tempered $2\frac{1}{4}$Cr1Mo steels

If the BN activity at higher currents corresponds to the second peak seen by Moorthy *et al.* (1997b) and attributed by them to unpinning of domain walls by carbides, then it appears that this activity is predominantly low-frequency noise. The other peak, occurring at a lower current and associated with unpinning from grain boundaries, is prominent at all frequencies. If the frequency is approximately the reciprocal of the 'time of flight' of the domain wall between pinning sites (Saquet *et al.*, 1999), then more closely spaced sites will produce noise of higher frequencies. When the applied current is small, the domain walls will be pinned by both weak and strong pinning sites, and the time interval between pinning events will be small. Increasing the current allows domain walls to bypass weaker pinning sites and move longer distances between events. If it is assumed that the domain wall velocity is approximately constant, then this would give noise of lower frequencies.

(Equation 5.15, however, gives the domain wall velocity as proportional to the difference between the applied field and H_C, so that walls would move faster at higher currents. Since this would tend to increase the frequency of events occurring at high currents, it appears that the jump size effect is dominant over the wall velocity effect in the system under investigation.)

Since it is believed that there is important information missing in these data sets as a result of filtering, it is not possible to interpret the signal shapes for the tempered steels with a great deal of confidence. However, the broadening of the peaks at higher temperatures and longer tempering times are indicative of a wider distribution of pinning site strengths, and the shift of the noise onset to a lower applied current after longer tempering corresponds to the appearance of weaker pinning sites.

8.4.2 11Cr1Mo steels

Steels designed for creep resistance contain, after tempering, a high concentration of fine alloy carbide particles to confer long-term microstructural stability. The high currents at which the peaks occur in this steel, and their similarity in shape to the AQ peak (Figure 8.12), suggest that little or no microstructural coarsening has taken place. This is borne out by an examination of the optical micrographs (Figure 6.16–6.19), which closely resemble the $2\frac{1}{4}$Cr1Mo steel in the very early stages of its tempering at 500 or 600°C.

Coarsening, with its associated loss of creep resistance, may be detectable in this steel by a shift of the noise onset to a lower current.

8.5 Conclusions

BN measurements were carried out on $2\frac{1}{4}$Cr1Mo and 11Cr1Mo steels tempered in a wide variety of conditions. In the $2\frac{1}{4}$Cr1Mo samples, some of the characteristics observed in previous work by Moorthy *et al.* could be seen; between the as-quenched and the tempered states the peak height increased, and its position moved to a lower current. Evidence of a second peak at higher current was present, but much suppressed by the hardware filtering, because it is composed primarily of noise with frequencies below the filtering

range of the system. Because of the difficulties in observing this second peak, detailed analysis of its relationship to tempering conditions and carbide sizes could not be carried out.

In the $2\frac{1}{4}$Cr1Mo samples, the maximum BN voltage occurs at a lower applied current with increasing Larson-Miller parameter. The 11Cr1Mo wt. % steel samples displayed peaks at a high current even after long-term heat treatment. It is believed that this is due to the coarsening resistance conferred by fine alloy carbides.

Measured BN data are very sensitive to experimental conditions such as frequency filtering and the shape and surface roughness of the yoke contact points and pickup coil core. This sensitivity may go some way towards explaining the discrepancies between results in the literature. Taking this into account, it would be advisable to develop a standard instrument and technique if BN measurements are to be used for safety-critical NDT applications.

Chapter 9 discusses the fitting of the model developed in Chapter 5 to these data sets.